Programming spatio-temporal patterns with DNA-based circuits

Marc van Der Hofstadt, Guillaume Gines, Jean-Christophe Galas, André Estévez Torres

Contents

Chapter 1

Programming spatio-temporal patterns with DNA-based circuits

Authors:. Marc Van Der Hofstadt[1], Guillaume Gines[2], Jean-Christophe Galas[1], André Estevez-Torres*[1]

1. Laboratoire Jean Perrin, Sorbonne Université and CNRS, 4 place Jussieu, 75005, Paris (France)

2. Laboratoire Gulliver, CNRS, ESPCI Paris, PSL Research University, 10 rue Vauquelin, 75005, Paris (France)

* andre.estevez-torres@upmc.fr

Common ways of computing do not use physical space to perform a single calculation[9]. However, in the physical world, and in particular in living systems, space has a major influence in the outcome of computations. In this chapter we will discuss DNA programs that take spatial inputs and compute spatial outputs. We will focus on systems that perform these calculations by reaction-diffusion, an important mechanism to describe the spatial behavior of large groups of molecules. We will first introduce basic concepts such as spatial

and analog computing and energy consumption in molecular computing. We will then briefly review the three current experimental implementations that allow to do so with DNA programs: DNA strand displacement, genelets and PEN DNA reactions. We will then discuss time-dependent spatial patterns that have been demonstrated with these systems, such as edge detection and traveling patterns. We will next make a survey of recent methods to control the parameters that influence the computation, in particular reaction and diffusion rates and boundary conditions. We will end by describing the design of steady-state patterns such as band patterns, which are relevant in early embryo development, and providing some perspectives for the future.

1.1. Introduction

1.1.1. What is spatial computing?

The majority of computations in everyday life are performed by microprocessors made of transistors. Within microprocessors, a computation is decomposed in operations that are carried out sequentially in time, thanks to a central clock. The spatial position of the input information or of the computing transistors does not influence the result. The opposite is true in many natural systems. For instance, groups of individual living agents use algorithms where the spatial position plays a crucial role. This is the case of herds of animals –such as birds or bees– where collective behaviors emerge from local interactions that are regulated by the behavior of nearby individuals[6]. It is also observed in developing embryos, where the final shape of the organism, but also the biochemical composition of each cell, depend on position. We thus define spatial computing

as any form of computation that is influenced by spatial coordinates, in particular because the physical process that performs the computation depends on space.

1.1.2. Digital vs. analog computing

Computing can be digital or analog. Digital computing works with discrete signals while analog computing operate with continuous ones. Digital and analog computing differ in two important points: the nature of the computing primitives and the propagation of noise[47]. In digital computing the primitives are based on the mathematics of boolean logic (AND, OR, etc.) and the integration of a large number of these primitives into a complex program is a science that can be rationalized and automated. In contrast, in analog computing the primitives are based on the physics of the computing system, such as the charge and discharge of a capacitor or the kinetics of a chemical reaction. Physical primitives have the advantage of being more efficient than boolean ones to perform a given calculation. However, combining physical primitives to perform complex calculations is an art difficult to rationalize and automate. This is a problem for engineers, but not for natural systems that have spent their evolutionary time trying out the most efficient ways to implement analog computations that are useful for survival.

DNA computing can also be digital or analog. An example of digital implementation are logic gates based on DNA strand displacement (DSD) reactions[52, 42]. However, spatial computations have mainly involved analog implementations whose computing primitives are given by chemical kinetics, and we will discuss them in section 1.2.

1.1.3. Computing consumes energy

Because any computation implies the transformation of a physical system it must consume energy. Energy supply is relatively straightforward in electronics through the use of power supplies. In molecular systems, computations are performed by chemical reactions and thus need 'chemical supplies' to run continuously. 'Chemical supplies' are ubiquitous in living systems —that is why we eat and breath— but are difficult to engineer in synthetic systems. The reason is that in electronics we have spatial separation through cables and we can thus use a single power supply that provides high voltage electrons for all the computing elements. In molecular systems, the computing reactions are all mixed in solution: they are thus connected through similar reactivities and isolated from each other using orthogonal reactivities.

Let's consider a series of orthogonal reactions $\mathrm{R}_i \rightarrow \mathrm{P}_i$ that are thermodynamically favorable (and thus their free energy change $\Delta_i G < 0$). A 'chemical supply' is a process that provides enough free energy to drive the conversion $\mathrm{P}_i \rightarrow \mathrm{R}_i$. Ideally, this recycling process is a chemical reaction that turns fuel F into waste W, $\mathrm{F} \rightarrow \mathrm{W}$, with an associated free energy change $\Delta_{cs} G < \sum_i \Delta_i G$. We thus need a single reaction that shares reactivity with many reactions that are orthogonal to each other, which is very hard to accomplish with the chemistry of small molecules. Nature solved this issue by evolving enzymes, large molecules that bear two (or more) orthogonal reactivities: one that is specific to a particular substrate and a second one that consumes a common fuel shared by a large set of enzymes, typically adenosinetriphosphate (ATP).

In DNA computing several solutions to this problem exist:

1. **One shot computations in a closed reactor:** In most implementations the reactants are mixed in a closed reactor without 'chemical

supply' and the solution can only perform a given computation once. This is the case of DSD logic gates[52, 42], for instance.

2. **Long transients in a closed reactor:** In some instances, the closed reactor contains a 'chemical supply'. In the case of strand displacement you cannot choose at the same time orthogonal sequences for the reactants (called gates, see below) and shared sequences for the fuels. The solution is thus to use as many fuel molecules as there are gates in the reaction[54]. DNA/enzyme computing systems, such as genelets and PEN reactions, use DNA hybridization to make orthogonal reactions and DNA-dependent enzymatic reactions coupled to an ATP-like fuel to implement a single 'chemical supply' that is orthogonal to the hybridization chemistry. If the fuel is consumed slowly compared with the time-scale of the computing reactions, such implementation can maintain the system out of equilibrium in a closed reactor for long enough to perform complex computations.
3. **Long transients in an open reactor:** Another way to implement a 'chemical supply' that recycles products back into reactants is to run the reactions in an open reactor that exchanges matter with the external world. An open reactor is physically connected to a source that flows in fresh reactants and to a sink that takes away the reacted mixture. This way, the reactor is constantly traversed by a free energy flow that keeps the system out of equilibrium.

1.1.4. Molecules compute in space through reaction-diffusion primitives

In this chapter we will review recent examples of spatial computations performed with DNA programs using reaction-diffusion primitives, because this mechanism is pervasive to reacting molecules in solution[30]. We will not discuss patterns created by DNA-programs in the absence of diffusion, such as those driven by self-assembly processes in DNA nanostructures, or patterned materials created from them, which are reviewed elsewhere[71, 22, 50], nor reaction-diffusion patterns generated by protein[33, 84] or transcription-translation networks[23, 57]. We further refer the interested reader to a recent review on pattern generation with DNA programs[67].

In the absence of space (for instance if the reactor is well mixed), the primitives of molecular computing are ruled by the kinetics of chemical reactions. For instance, the reaction of two single-stranded DNA (ssDNA) A and B to give the double strand C is written

$$\mathrm{A} + \mathrm{B} \underset{k_2}{\overset{k_1}{\rightleftharpoons}} \mathrm{C} \tag{1.1}$$

where k_1 and k_2 are the hybridization and dehybridization kinetic rate constants, respectively. Supposing mass-action law kinetics, the temporal evolution of the concentration of species C is given by

$$\frac{\mathrm{d}C}{\mathrm{d}t} = k_1 A \cdot B - k_2 C \tag{1.2}$$

where the concentration of a given species is noted in italics. Eq. 1.2, together with similar equations for species A and B, are the computing primitives of a

bimolecular reaction.

In the absence of mixing, the transport of each species by diffusion must be taken into account. For instance, in a one-dimensional (1D) reactor the spatiotemporal evolution of C involved reaction 1.2 is given by

$$\frac{\partial C}{\partial t} = k_1 A \cdot B - k_2 C + D_C \frac{\partial^2 C}{\partial x^2} \tag{1.3}$$

where D_C is the diffusion coefficient of species C and x the spatial coordinate. Eq. 1.3, together with the corresponding equations for A and B, are the primitives for the reaction-diffusion dynamics of a bimolecular reaction.

In the general case where n reactive species form a reaction network characterized by the reaction matrix F, reaction-diffusion dynamics are given by

$$\frac{\partial u_i}{\partial t} = F_i(u_1, \ldots, u_n) + D_i \frac{\partial^2 u_i}{\partial x^2}, \qquad i = 1, \ldots, n, \tag{1.4}$$

where u_i is the concentration of species i and D_i its diffusion coefficient. The term reaction-diffusion was coined by Alan Turing in his seminal work *The chemical basis of morphogenesis*[61]. The interest of reaction-diffusion (RD) systems is that they make emerge a spatial distance $\lambda = \sqrt{D/k}$, where k is a first order rate constant characteristic of the reaction kinetics and D a diffusion coefficient[39]. Reaction-diffusion is thus a convenient way of computing distances that depend on chemical inputs and that provide chemical outputs. Under some circumstances[13, 39], a system obeying Eq. 1.4 generates spatial structures of wavelength λ, namely

- edge detectors;
- traveling fronts, waves and spirals;
- Turing patterns; and

- stationary fronts and band patterns.

All these patterns have been observed and investigated, principally between 1970 and 2000, with reactions based on the redox chemistry of small molecules, of which an archetypal example is the Belousov-Zhabotinsky (BZ) oscillator[14]. However, redox chemistry is not programmable and its harsh acidic conditions make it incompatible with biological materials. Engineering RD patterns with DNA programs solves these two issues. In sections 1.3 to 1.4 we will see how these patterns —except Turing ones— have been engineered with DNA programs.

1.2. Experimental implementation of DNA analog circuits

In this section we discuss the three DNA-based experimental systems that can currently perform analog computations coupled to a 'chemical supply' and that are thus amenable to non-trivial reaction-diffusion computing: DNA strand displacement, genelets and PEN reactions. We review them by showing how to implement a cornerstone of non-equilibrium dynamics: a chemical oscillator.

1.2.1. DNA strand displacement oscillators

Toehold-mediated DNA strand displacement was developed by Yurke, Turberfield and collaborators as a way to use ssDNA as a catalyst to fuel DNA-based nanomachines[73, 59]. Their simple and powerful idea was to control the kinetics of dsDNA dehybridization through a hybridization event: if the partially

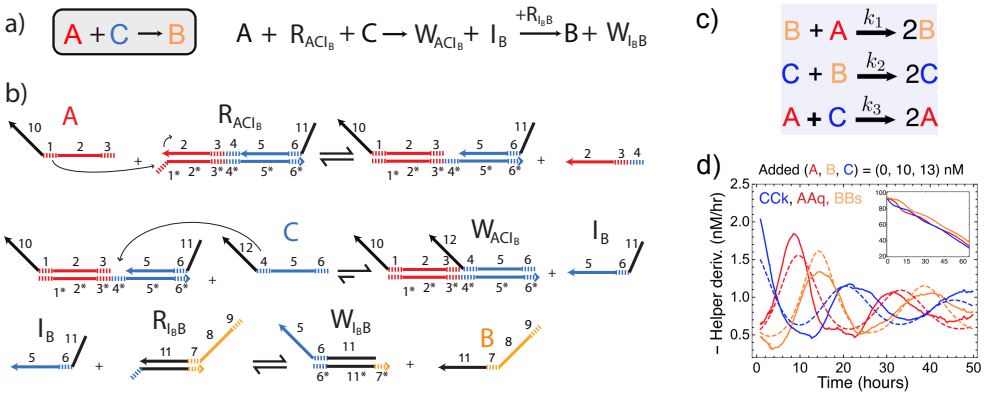

Figure 1.1: Principle of DNA strand displacement (DSD) reactions (a-b) and oscillations in a DSD circuit in a closed reactor (c-d). a-b) DSD implementation of the reaction kinetics A+C → B. The reaction needs the reaction gates R_{ACI_B} and R_{I_BB} that act as fuels and are converted into waste W_{ACI_B} and W_{I_BB} (a). b) Detailed mechanism of the reaction in (a): ssDNA are noted as arrows, the 3' end being at the tip of the arrow. Sequence domains are indicated by numbers and an asterisk * denotes their complementary sequence. Toeholds are represented as dashed lines. c) Formal reaction mechanism of the DSD rock-paper-scissors oscillator. d) Experimental results showing oscillations of the network in panel (c) in a closed reactor (solid lines: experimental data, dashed lines: model fits). Panels (c-d) adapted with permission from ref. 56 (see also ref. 55).

double-stranded complex t:b carries a dangling end on the bottom strand b, then the dissociation of the top strand t is significantly faster in the presence of strand b*, fully complementary to b, because b* may hybridize to the dangling end of t:b, called toehold, and eject t by strand displacement. This strategy introduces two new features compared to standard DNA hybridization between fully complementary sequences: i) one can quantitatively control the rate of production of species t by up to six orders of magnitude by changing the length or the position of the toehold[81, 19], and ii) every DNA strand displacement (DSD) reaction can be used to generate a new toehold that may subsequently react, thus opening the path to using ssDNA as a building block

of chemical reaction networks.

Although DSD reactions were first applied to digital computing by Winfree and collaborators[52, 42, 82] they can also be used in analog computations. This was first proposed theoretically in 2010[54] and recently demonstrated experimentally by synthesizing a DSD oscillator[55]. To design DSD analog computations, one first chooses a suitable formal mechanism. As an example, let's consider the bimolecular reaction A + C $\rightarrow$ B. Species A, C and B are encoded with ssDNA strands composed of a species-specific and a reaction-specific domain (respectively colored and black in Fig. 1.1a). The reaction is implemented in two steps with two gates R_{ACI_B} and R_{I_BB} (Figure 1.1a), which are DNA complexes composed of two or more partially-hybridized DNA strands bearing reactive toeholds. First, the step A + C $\rightarrow$ I_B is implemented by R_{ACI_B} that is an AND gate that produces intermediate I_B in the presence of both A and C. A second gate R_{I_BB} takes the released species I_B as an input and produces B.

Autocatalytic reactions of the type A + B $\rightarrow$ 2A can be experimentally implemented by using a gate that takes two different inputs and generates two identical outputs[55]. The leak inherent to any autocatalytic reaction may be efficiently suppressed by adding a thresholding module that suppresses the output that detaches from the gate in the absence of the input. By connecting three of these autocatalytic modules that repressed each other, Srinivas, Soloveichick and collaborators[55] succeeded the tour-de-force of synthesizing a DSD oscillator in a closed reactor, thus proving for the first time that complex analog networks with feedbacks can be built and kept out of equilibrium with DSD reactions (Figure 1.1b).

1.2.2. DNA/enzyme oscillators

DSD networks have the advantage of being fully programmable, however up to 7 DNA species are needed to implement a single autocatalytic node[55], 4 of them being fuel molecules, which increases the number of control parameters to be optimized to obtain the desired dynamics. A way to circumvent this problem is to use enzymes that catalyse the conversion of an input into an output strand and that use a common fuel that is orthogonal to DNA hybridization chemistry. In this regard, a powerful idea is to emulate what happens in gene regulatory networks, where genes produce protein transcription factors, TFs, that increase or reduce the rate of production of other TFs, all being degraded by a specific enzyme.

This idea was first implemented in 2006 by Kim and Winfree[27], who built a bistable network and later an oscillator[28]. To do so, they combined DNA and RNA strand displacement reactions with transcription and RNA degradation assisted by two enzymes, RNA polymerase and RNAse. This reaction framework receives the name of genelet. A similar idea was implemented in a different manner by Rondelez and co-workers who built a three-node relaxation oscillator[37] and later a predator-prey oscillator[17] and two bistables[40, 38]. For this they used short DNA strands and three enzymes, a polymerase, an exonuclease and a nicking enzyme, in a reaction framework called PEN DNA toolbox (PEN stands for the first letters of the three enzymes involved).

1.2.2.1. Genelets

Genelets are constituted of three types of nucleic acid species (Figure 1.2a). Nodes, O_i, are RNA strands that are created and degraded, and thus play the role of TFs. Switches, S_{ij}, are partially dsDNA species that may create nodes

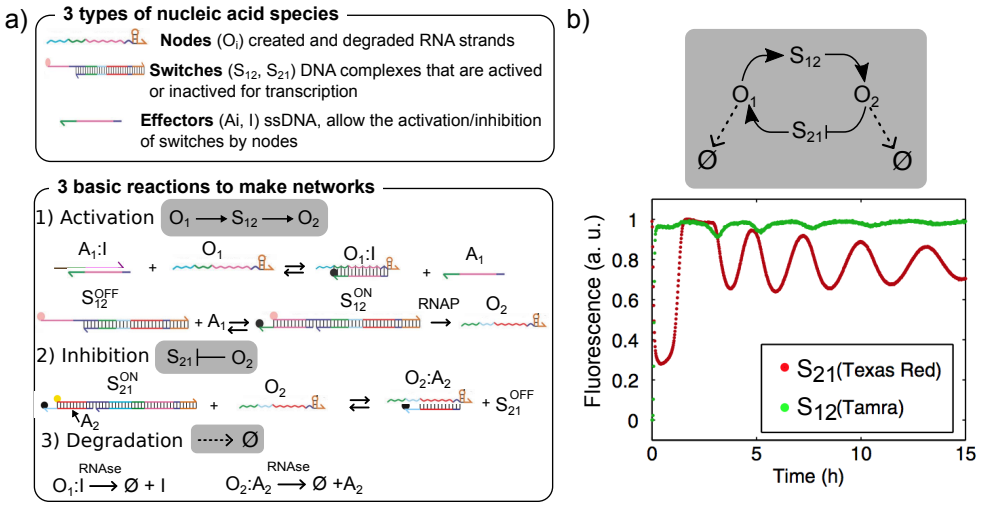

Figure 1.2: Mechanism of the genelet reaction system (a) and network oscillating in a closed reactor (b). Harpoon arrows denote ssDNA, curly arrows refer to RNA, colors indicate sequence domains, similar colors indicating complementary sequences. RNAP stands for RNA polymerase. Adapted from ref. 28.

by transcription depending on their activity state, and are thus equivalent to genes. Effectors, A_i and I, are ssDNA species that make the link between nodes and switches. To construct networks with genelets, one needs to modulate the activity of switches S_{ij} with input nodes O_i, which is performed by a combination of strand displacement and transcription reactions.

In its off state, noted S_{ij}^{OFF}, a switch carries an incomplete RNA polymerase (RNAP) promoter sequence, and is thus inactive for transcription. S_{ij}^{OFF} is activated in the presence of A_i that binds to S_{ij}^{OFF} and completes the RNAP promoter sequence, generating species S_{ij}^{ON}. In Figure 1.2, inhibition of S_{21}^{ON} by O_2 is directly made by the hybridization of O_2 with strand A_2 on S_{21}^{ON}, generating S_{21}^{OFF} and making the partial DNA duplex O_2:A_2. Activation of S_{12}^{OFF} by O_1 is made through the intermediary of complex A_1:I. O_1 reacts with A_1:I and liberates A_1 that activates S_{12}^{OFF}. In the presence of RNAseH,

which specifically degrades RNA hybridized to DNA, species O_1:I and O_2:A_2 continuously regenerate I and A_2 and destroy the nodes O_i. The production of RNA by consuming nucleotidetriphosphates, NTPs, and its degradation through RNAse ensure that the network is kept out of equilibrium for 10-15 hours in a closed reactor. Genelets have been used to construct bistable[27, 51] and oscillatory networks[28, 16].

1.2.2.2. PEN reactions

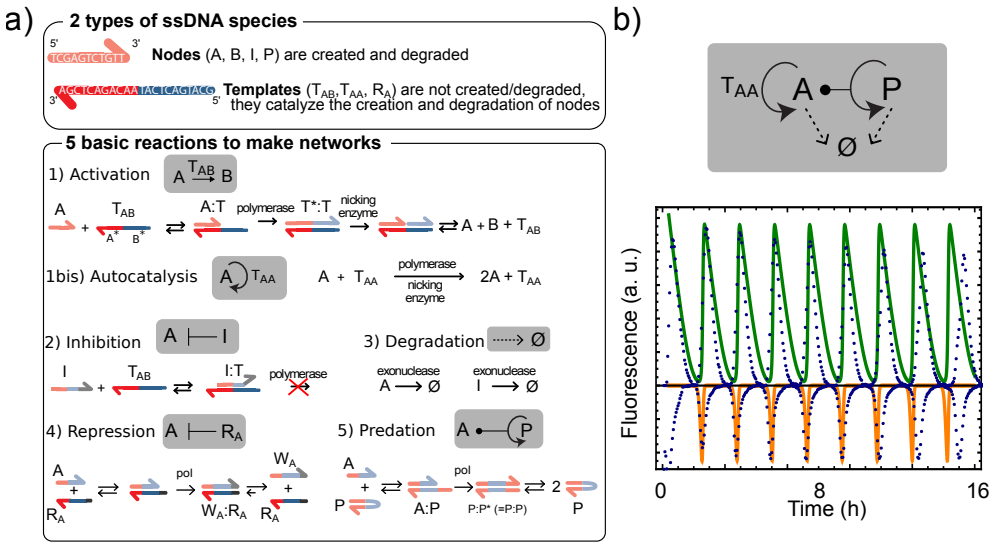

Figure 1.3: Mechanism of the PEN DNA toolbox reaction system (a) and network oscillating in a closed reactor (b). a) Harpoon arrows denote ssDNA, colors indicate sequence domains, similar colors indicating complementary sequences. b) PEN toolbox predator-prey oscillator. Topology of the reaction network (top) and experimental data (dots) and fits to a 2-variable model (lines). P appears in green and A in orange. Panel b displays data related to ref. 17.

PEN reaction networks are assembled with two types of species (Figure 1.3a). Templates, T_{ij} are ssDNA species that carry the information about the topology of the network and their concentrations do not change over time; they

are equivalent to genes. Nodes (A, B, I) are shorter ssDNA strands that are processed and created by the templates, they are both produced and degraded over time; they play the role to TFs. These two species, together with 3 enzymes, can perform five types of reactions in the presence of dNTPs: activation, inhibition, degradation, repression and predation.

Template T_{AB} catalyses the activation reaction $A \rightarrow A + B$, where A and B are nodes. T_{AB} is typically 20-25 nt-long and it carries two sequence domains, the input domain, of sequence A^*, and the output domain, noted B^*, respectively complementary to A and B. Nodes are typically 10-15 nt-long. During activation, A binds to the input site of T_{AB} to form species A:T_{AB}, which is extended by a DNA polymerase, pol, into dsDNA species T^*_{AB}:T_{AB} (T^*_{AB} has the sequence A–B). A nicking enzyme, nick, recognizes a 5 or 6 nt-long sequence on T^*_{AB}:T_{AB} and cuts the upper strand T^*_{AB} between domains A and B, which dehybridizes into species A, B and T_{AB}. The temperature is chosen in the range 37–45^o such that the complex A:T_{AB} is close to the melting temperature but T^*_{AB}:T_{AB} is stable. Autocatalysis can be encoded in an activation template T_{AA} whose input and output domains are identical. Note that, as it happens with any autocatalytic reaction, PEN autocatalysis 'leaks', i.e. it starts in the absence of input A, because the polymerase is able to synthesize A in the absence of template[86]. In standard conditions this leak happens within 100 min, but it can be simply reduced in the presence of high concentrations of nicking enzyme to reach 10 h, and even totally suppressed in the presence of repression (see below), which turns the monostable autocatalytic node into a bistable one[38]. A second side-reaction of PEN autocatalysis is the generation of autocatalytic parasites, which result from untemplated autocatalysis[86]. This reaction generates mixtures of DNA strands

spanning ten to several thousands nucleotides that ultimately break the designed dynamics of PEN networks at long times. Depending on the conditions, parasites emerge after 5 to 50 h. However, these parasites may be suppressed from functional PEN networks by adopting a three-letter encoding[63].

Inhibition of T_{AB} is performed by strand I, typically 15 nt-long, that partially hybridizes to domains A^* and B^* on T, forming I:T. A single-stranded overhang on the 3' end of I bound to T_{AB} precludes the polymerase to extend it, and a careful choice of its sequence, prevents nick from cutting it. Degradation of nodes is performed by a single-stranded DNA exonuclease that does not degrade templates because they are chemically modified on their 5' end. Repression of an autocatalytic node can be implemented by adding a template R_A that takes A as an input and adds a short sequence to its 3' end, converting it into a waste product, W_A, unable to react with the template T_{AA}. In this configuration, when R_A is a degradable node with palindromic sequence, noted P, a predation reaction of the type $A+P \rightarrow 2P$ can be implement. To construct a network, activating and inhibiting links are selected such that the sequence of output B is, respectively, the input or the inhibitor of a downstream template. The continuous production and degradation of node strands, which consumes deoxynucleotidetriphosphates, dNTPs, keeps the network out of equilibrium in a closed reactor.

The PEN toolbox has produced so far oscillators that are significantly more robust than those reported using genelets (Figures 1.2b and 1.3b). The two- and three-node genelet oscillators[28, 16] oscillate for 6 periods during 20 h and for 3 periods during 15h, respectively. In contrast, the two-node predator-prey[17] and the three-node oligator[37] PEN oscillators oscillate for 26 periods for 32 h and for 18 periods during 30 h, respectively. Unpublished results with

Table 1.1: Principal characteristics of the three experimental systems capable of reaction-diffusion computations with DNA. Programmable and non-programmable sizes refer to the number of bases of the elements that can be designed or not in the different implementations (non-programmable corresponds to enzymes), extracted from [55]. The time-scale and the life-time correspond to the typical period and duration of the oscillations in a closed reactor. Types of temporal and spatial patterns experimentally implemented with each system. Numbers in brackets point to references.

	DSD	Genelets	PEN toolbox
Programmable size (nt)	1386	469	71
Non-programmable size (bp)	0	~ 4000	~ 7700
Time-scale (h)	20[55]	3[28]	1.5[17]
Life-time (h)	50[55]	20[28]	80[18]
Temporal pattern	Autocatalyst[83], oscillator[55]	Bistable[27, 51], oscillator[16, 28]	Autocatalyst[37], bistable[40, 38], oscillator[37, 17], chaos[17], excitable[38]
Spatial pattern	Edge-detection[8], linear gradient[80], band pattern[80]	Traveling front[53], pulse[12]	Traveling front[75, 78], wave[41] and spiral[41]; go-fetch front[20]; band pattern[76, 62]; french flag pattern[76], colony formation[20]

the predator-prey oscillator demonstrate more than 100 periods for more than 130 h. The reason of this greater robustness may be attributed to a cleaner degradation mechanism in the PEN system; while RNAse H only partially degrades RNA strands, the DNA exonuclease used in PEN reactions transforms the nodes into single nucleotides, reducing inhibition by degradation products. Table 1.1 recapitulates the properties of the three analog implementations reviewed here and summarizes, to the best of our knowledge, the temporal and spatial patterns obtained with them.

1.3. Time-dependent spatial patterns

In this section we review experimental realizations of spatial calculations which output is a spatial concentration pattern that depends on time. We will first see how an incoherent feed forward loop network performs edge detection and how an autocatalytic program generates propagating concentration fronts. We will then describe go-fetch fronts that are able to interrogate the presence of a particular DNA sequence at a distance, and traveling waves and spirals based on DNA oscillators. Finally, we will review methods to control the diffusion coefficient and the geometry of the environment where the spatial pattern evolves.

1.3.1. Edge detection

Reaction-diffusion programs can perform some image-processing algorithms where the input and output are images encoded as concentration patterns. This was first demonstrated using the Belousov-Zhabotinsky reaction in 1989[31]. In 2013, Chen, Ellington and co-workers engineered DNA reaction networks that detected the edge of an input image (Figure 1.4)[8]. The computation was performed by a reaction network where the input I comes in the form of light, and A, B and C are DNA strands. On the one side, I activates A and triggers the cascade A $\rightarrow$ B $\rightarrow$ C. On the other side, I inhibits B and thus inhibits de cascade B $\rightarrow$ C. Because I activates and inhibits C, such network is called an incoherent feed forward loop (IFFL). In addition, A needs to diffuse faster than B and C. Let's now consider that we illuminate the medium with a pattern with a border between light and no light (1/0, Figure 1.4a). The illuminated zone will produce A and destroy B, and thus no output C will be observed in

this zone. The dark zone will not produce A nor B, but A will diffuse across the border from the illuminated zone and react with B, producing C at the border between the two zones. The low diffusion of B and C makes the generated concentration profile of C sharper.

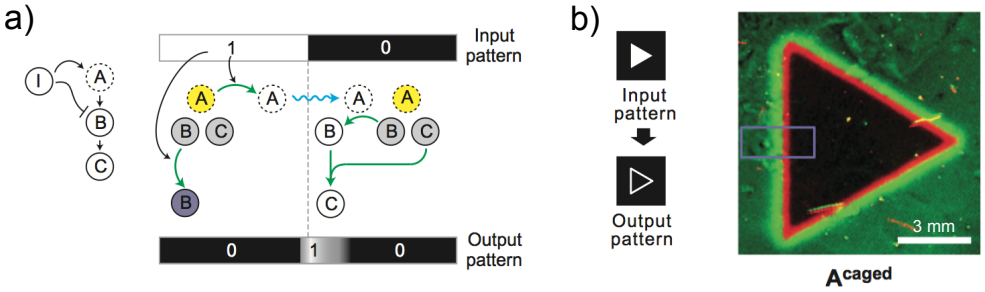

Figure 1.4: Reaction-diffusion edge-detection pattern engineered with DNA strand displacement circuits. a) Mechanism of the incoherent feed-forward loop (IFFL) DNA network. Light is denoted as the input species I and the only fast-diffusing species is A. A and B are photoresponsive DNA strands that, upon illumination, break into two strands, inactive B uncapable of producing C in the illuminated area, and active A that diffuses into the non-illuminated area and activates B and fluorescent product C, creating the highlighted edge. b) Fluorescent pattern obtained when flashing light with a triangular shape in a gel filled with an IFFL DNA network. Reprinted by permission from Springer Nature, Nature Chemistry, [8], Copyright 2013.

The authors implemented this program by converting the input light pattern into DNA concentration through caged DNA strands containing a photocleavable nitrophenyl amide spacer. The network was based on the catalysed hairpin assembly (CHA) reaction[72], that is related to DSD but implements gates using hairpins, instead of duplexes. For instance, A was an unreactive hairpin that was cleaved by UV light and formed a reactive ssDNA. In contrast, B was a reactive hairpin whose toehold was cleaved by light, yielding an unreactive species. Figure 1.4b shows the experimental output pattern in red. Note that, because there is no 'chemical supply' in this implementation, the

output pattern is transient and will fade away by diffusion after some time. To our knowledge, this was the first experimental demonstration of RD patterns programmed with DNA.

Complementary to edge detection, Abe et al. demonstrated the computation of a line segment equidistant from two source points[1]. These experiments were also performed in a gel matrix. A DNA logic AND gate was anchored everywhere in the gel, and two holes made in the gel were filled with the gate inputs. Both inputs diffused through the matrix, and activated the AND gate only at the equidistant region from the source points; thus producing a Voronoi pattern. More complex patterns were observed when multiple source points were involved.

1.3.2. Traveling patterns

In the absence of reaction, the diffusion of a chemical species is quite boring: a concentration profile will fade away until reaching a spatially homogeneous final state, following Fick's diffusion law. In contrast, in the presence of an autocatalytic reaction, which is a transformation where the product catalyses its own production, an inhomogeneous concentration profile will generate concentration patterns that propagate, often with constant velocity. Traveling patterns are an efficient way to convey chemical information across distances where diffusion is too slow.

1.3.2.1. Fronts

The simplest traveling pattern is the front (a structure with a single low-to-high concentration transition) that just needs a single autocatalytic loop, which we

can simply write

$$A \xrightarrow{k} 2A \tag{1.5}$$

where k is the reaction rate. The first observation of a traveling front of concentration was reported by Luther in 1906[35] (translated in [36]), in a redox reaction. Luther proposed an expression for the velocity v of propagation of the front that is still valid,

$$v = a\sqrt{kD}, \tag{1.6}$$

where a is "a constant between 2 and 10", k the rate constant of the autocatalytic reaction and D the diffusion coefficient of the autocatalyst. Luther's formula may be obtained by an order of magnitude argument. Let's consider an autocatalytic species A initially distributed along a 1-dimensional reactor with a front concentration profile. Let's define the characteristic time of the autocatalytic reaction $\tau_{chem} = 1/k$. The distance traveled by diffusion during this time is $l_{diff} = 2\sqrt{D\tau_{chem}}$. For times shorter that τ_{chem}, A at the tip of the front diffuses and does not react. For times longer than τ_{chem}, the autocatalytic reaction amplifies A until saturating all the regions where A has diffused, regenerating an identical front ahead of the initial one. The velocity of such a front is thus $v \sim l_{diff}/\tau_{chem} = 2\sqrt{kD}$. The grounds for the theory of traveling fronts were independently developed by Fisher[15] and by Kolmogorov, Petrovsky and Piscounov[29] in 1937. In particular, $v = 2\sqrt{kD}$ is exact for a single-variable RD system following Eq. 1.4 with a reaction function $F(u)$ that is monostable and verifies $F(u)/u < F'(u)$[65]. Such systems are called Fisher-KPP fronts. The interested reader may refer to refs. 39, 64, 44, 65.

In 2015, Zadorin and collaborators demonstrated that programmable traveling fronts could be obtained with PEN autocatalysers[75]. The autocatalytic

behavior of node A growing on template T_{AA} is demonstrated in Figure 1.5a, where the concentration of A:T_{AA} is measured by fluorescence in the presence of a DNA intercalator and plotted *vs.* time. At short time (and thus low A) the system behaves as $A = A(0)e^{kt}$, where k is the rate constant of autocatalysis.

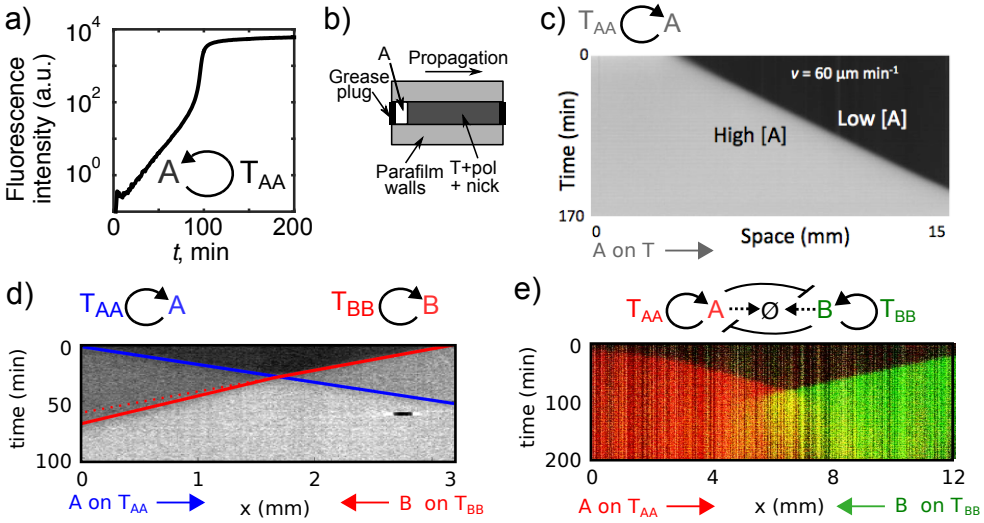

Figure 1.5: PEN autocatalysers generate programmable concentration fronts that travel at constant velocity. a) Temporal dynamics of a simple PEN autocatalyser. The log-lin plot shows DNA intercalator fluorescence proportional to the concentration of A, the initial linear slope indicates exponential growth. b) Sketch of the experimental setup to observe fronts. c-e) Kymographs of the fluorescence signal for different autocatalytic networks show a single front (c) and two counter-propagating fronts that either do not interact (d) or that strongly inhibit each other (e). Panels b and d reprinted with permission from [75] Copyright 2015 by the American Physical Society.

In a one-dimensional reactor such as the one depicted in Figure 1.5b — filled homogeneously with a solution containing an T_{AA}, pol, nick and dNTPs, and containing an excess of autocatalytic node A on the left-hand-side— a front propagating with uniform velocity, typically 60 μm min^{-1}, was observed through time-lapse fluorescence microscopy (Figure 1.5c). To check if the front followed Luther's equation 1.6, the velocity of the front was measured for dif-

ferent reaction rates k and different effective diffusion coefficients D. The rates were controlled by changing the concentration of the template T_0 (in a certain concentration range, $k \sim T_0$ in PEN reactions), while D was reduced by attaching a hydrodynamic drag to the template strand (see below). In all these cases, the measured velocities followed Luther's scaling $v = a\sqrt{kD}$ with $a = 2.6$, both for k and D.

The programmability of this approach was illustrated by designing different networks containing autocatalysis that resulted in controlled spatio-temporal dynamics. Two autocatalysts with orthogonal sequences generated fronts that cross-propagated with little interaction (Figure 1.5d). In contrast, two autocatalysts that cross-inhibited themselves created repelling cross-propagating fronts (Figure 1.5e).

Note that traveling fronts have not yet been demonstrated with DSD networks even if autocatalytic networks exist[83, 72]. A possible reason is that it is more difficult to control the leak of DSD autocatalysts compared to PEN ones. Indeed if the autocatalytic reaction leaks, the area ahead of the front will get triggered before the front arrives and homogeneous amplification will be observed. However, considering that CHA autocatalysts may remain untriggered for 3 h[72] and recent DSD autocatalysts are stable for tens of hours[55], DNA-only traveling fronts may soon be observed. Finally, autocatalytic fronts have also been observed in genelet networks[53], although it remains to be tested that they verify Luther's formula.

1.3.2.2. Go-fetch fronts

The above-mentioned spatiotemporal reaction networks operate with species that freely diffuse in solution. It may also be possible to localize the reaction by

grafting the catalysts on different positions of a substrate. For instance, Gines et al. used particle-bound DNA strands to spatialize the chemical reactions in a fluidic chamber[20]. Here, the DNA templates were grafted via a biotin-streptavidin linkage onto micrometric hydrogel particles, which results in the localized production of output strands on the particles, while the degradation happens in the whole reservoir.

Particles bearing a PEN autocatalyser generated a traveling front of constant velocity. In addition, the authors reported a 'go-fetch' chemical system that computes the distance between two specific DNA sequences through two orthogonal traveling fronts (Figure 1.6a). This experimental implementation uses 4 populations of DNA-programmed particles. The sender (S_A) initiates the production of strand A on the left side of the channel using a —leaky— monostable autocatalytic loop. A first relay population (R_A), grafted with a bistable switch that amplifies A, transmits the signal across the chamber. When the signal A comes across the receiver particle (C_{AB}), placed on the right side of the channel, it activates the production of strand B. This reaction is catalysed by an activation template T_{AB} that converts A into B. B finally propagates through the second relay population (R_B) until reaching S_A, which in turn exhibits a fluorescent signal. This system is programmed to compute the distance between S_A and C_{AB}, which correlates with the time it takes to the S_A particles to fluoresce upon receiving the B strand. Interestingly, RD enables long-distance communication ($\sim$ 1cm), which is at least 3 orders of magnitude larger than the particle size (~ 10 μm). A limitation of this protocol is that the particles are randomly distributed in a microchamber, with a poor control on the localization of the reactants. It would be interesting in the future to implement the precise disposition of particles programmed with dif-

ferent sensing networks and build on these organized arrays to create tissue-like systems.

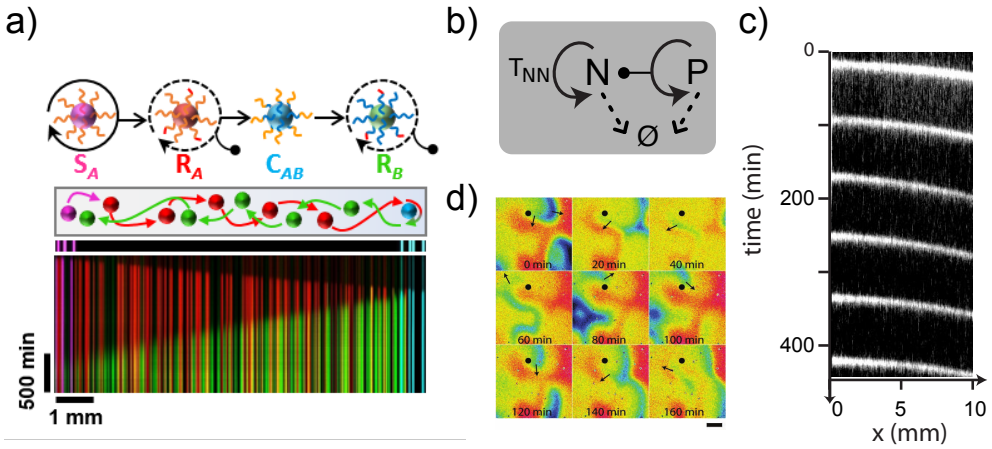

Figure 1.6: 'Go-fetch' fronts (a) and waves and spirals with PEN reactions (b-d). a) A 'go-fetch' program is implemented when PEN template strands are attached to microparticles distributed in 4 populations: S_A = sender particle, R_A and R_B = relay particles, C_{AB} = converter particles. When the signal A transported by R_A reaches C_{AB}, it is converted to B that travels back transported by R_B to the initial position (top). The bottom kymograph represents the go front in red and the reply front in green. b) Topology of the PEN predator-prey (PP) network. c) Kymograph of prey fluorescence in a 1-dimensional reactor. Oblique white lines correspond to traveling waves. d) Time-lapse fluorescent images of a prey (N) spiral turning around the black dot (false color). Panel (a) reprinted by permission from Springer Nature, Nature Nanotechnology, [20], Copyright 2017. Panels (c,d) adapted with permission from [41]. Copyright (2013) American Chemical Society.

1.3.2.3. Waves and spirals

An autocatalytic loop coupled to a delayed inhibition makes an oscillator that, in the presence of diffusion, creates chemical waves and spirals that travel at constant velocity[13]. Such patterns have been observed in the BZ oscillator in the early 70s [77, 68] but have only recently been observed in DNA systems

with the PEN predator-prey (PP) oscillator[41].

The mechanism of the PP oscillator is simple and produces robust oscillations[17] (Figure 1.3b). Species N, the prey, grows autocatalytically on template T_{NN}. The trick is that species P, the predator, is both palindromic, *i.e.* it is self-complementary, and contains the sequence of N (Figure 1.3a). When P and N bind together, the polymerase extends N, yielding two P, and thus P grows autocatalytically consuming the prey ($N + P \rightarrow 2P$). In addition N and P are both degraded, mimicking the natural decay of preys and predators.

When a spatial reactor was filled with the PP mixture and the initial concentrations of N and P were homogeneous, traveling concentration waves of prey, followed by predator waves were observed[41] (Figure 1.6c). The wave velocities were in the range $80 - 400$ μm min^{-1} and were in fair agreement with a 2-variable model related with Eq. 1.6. When the initial condition of prey was inhomogeneous, spirals were observed (Figure 1.6d). This was the first report of traveling waves in a chemical reaction network built from the bottom up. It was also the first observation of predator-prey waves in the laboratory.

1.3.3. Controlling spatio-temporal patterns

We have seen in section 1.1.4 that the output of a reaction-diffusion computation is given by the solution to the system of partial differential equations in Eq. 1.4. Such solution depends on four important features:

1. the topology of the reaction network, i.e. the function F in Eq. 1.4,
2. the reaction rates,
3. the diffusion coefficients,

4. the initial and boundary conditions.

We have just discussed some network topologies that provide different outputs: an incoherent feed forward loop (IFFL) that makes an edge detector or an autocatalytic node that generates a traveling front, for instance. We have also seen that reaction rates can be changed in DSD reactions by changing the length of the toehold and in PEN reactions by tuning the concentration of the template strands. Here we further discuss strategies to control diffusion coefficients and initial and boundary conditions.

1.3.3.1. Controlling diffusion coefficients

The first strategy for reducing D is to increase the viscosity of the solution by adding a viscous solute such as glycerol or polyethyleneglycol. The drawback is that this method is not specific and all DNA species will be slowed down by a similar factor. The second strategy is to perform the reaction inside a sieving matrix, like a hydrogel, such that large DNA species will be trapped and small ones will diffuse freely. This method was successfully used in the edge detection network discussed above[8]. In this case the fast-diffusing strand A was shorter than the other reagents (8 vs. 64 nt. long) and reactions were performed in 20% crosslinked polyacrylamide gel, resulting in a striking 10-fold difference in diffusion coefficient. The last strategy is to specifically change D for a given species, which can be performed by attaching a DNA strand to a hydrodynamic drag. This method was employed to modify the diffusion of PEN autocatalysers, the drag being a triton micelle of $\sim$ 5 nm radius to which a cholesteryl-modified template T_{AA} was attached (Figure 1.7a). Autocatalyser A needed to bind to T_{AA} to grow and, depending on the molar fraction of cholesteryl template, D was reduced up to 2.7-fold[75]. Importantly, not only

the effective diffusion of a passive solution was controlled but also the one of A involved in a reaction-diffusion front, which was demonstrated by measuring the velocity of the front.

An improved hydrodynamic drag was demonstrated by Rodjanapanyakul et al. by using a linear copolymer of polyacrylamide and strand T [43], reaching a reduction of D of 5-fold in DSD reactions, an approach also modeled by Allen et al.[3]. With this stratefy the effective diffusion of freely-diffusing strand A, complementary to T, could be modulated by changing the concentration of a competitor strand C that also bound to T (Figure 1.7a,b)[43]. A similar strategy was used to control the electrophoretic mobility of DNA involved in DSD programs[2]. Recently, the copolymerization of DNA with polyacrylamide was used to stablize PEN static RD patterns for more than 60 hours[62].

1.3.3.2. Initial and boundary conditions

In the aforementioned examples, the initial condition, or input signal, was introduced either by adding a droplet of solution containing the input species, which results in poor spatial resolution, or by using a light pattern, with high spatial resolution. Other ways of controlling the initial condition include microfluidic injection using PDMS monolithic pumps[78] and electric switches[32]. In this last example, Kurylo et al. grafted an oligonucleotide on gold electrodes embedded in microfluidic channels. They took advantage of the electrochemical properties of the thiol-gold bond to release specific DNA localized in space and time through a voltage pulse. In particular, the DNA release was able to trigger PEN autocatalytic fronts. Without involving delicate liquid handling, this method offers the possibility to control and interact in real time with running DNA-based molecular systems.

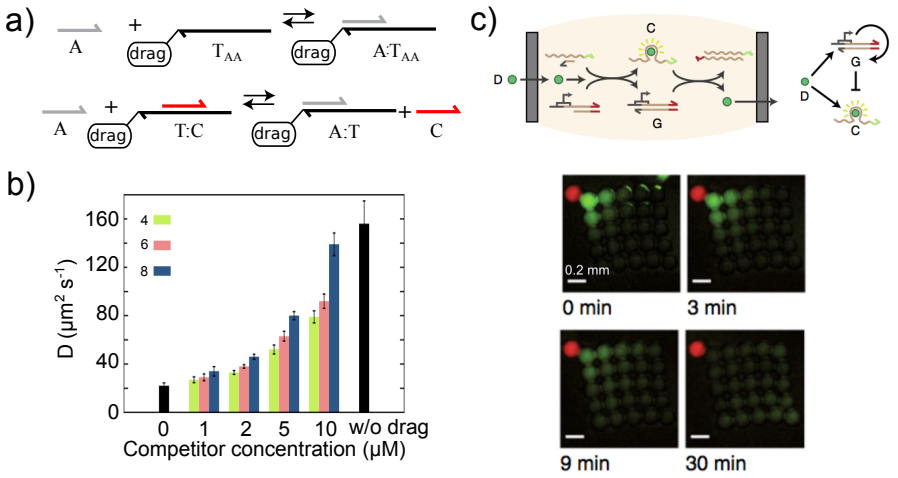

Figure 1.7: Strategies to control the diffusion and geometry of RD patterns. a) Two methods to tune the diffusion of strand A proposed in [75] (top) and [43] (bottom). b) Diffusion coefficient of species A measured for the competitor strategy in panel (a), bottom, for different competitor concentrations. The colors refer to different lengths of the toehold where A binds on T:C. Reprinted figure with permission from [43] Copyright 2018 by the American Physical Society. c) An incoherent feed forward loop genelet network (top) processes information from DFHBI green fluorophore, D, present in the red droplet (bottom) across a square array of droplets bearing protein nanopores and generates a diffusion pulse (from the red droplet on the top left corner to the bottom right corner droplet). Reprinted by permission from Springer Nature, Nature Chemistry, [12], Copyright 2019.

The simplest way to control boundary conditions in a reaction-diffusion process is to change the geometry of the reactor where the process takes place. This can be performed with standard microfabrication methods, although one has to take care to choose a material that limits evaporation, which is particularly important for PEN reactions that occur in the temperature range 37-45°C. To this end, NOA microfluidic devices[4] were used to investigate the effect of curvature in the propagation dynamics of PEN autocatalysers and to demonstrate that DNA-based pulses can compute the optimal path within a maze[78].

An interesting alternative for controlling the geometry of RD patterns was proposed by Dupin and Simmel[12] (Figure 1.7d). They distributed a genelet reaction network inside a 2-dimensional array of microdroplets that were interconnected by protein nanopores. These nanopores allowed the droplets to exchange DFHBI, a small molecule that fluoresces when bound to the spinach RNA aptamer, but hindered the DNA-program from leaving the DNA-impermeable droplets. By constructing an IFFL reaction network that takes DFHBI as an input and produces the spinach aptamer as output, a transient pulse of fluorescence across an array of droplets was observed in the presence of a seed droplet with high concentration of DFHBI; which was reported both in 1 and 2 dimensions. With this clever idea, the authors obtained compartments that displayed a certain degree of autonomy, and at the same time the capability to exchange and process specific chemical information, mimicking cell-cell communication in living tissues. For the moment, the messaging molecule, DFHBI, cannot be amplified autocatalytically, and thus the propagation velocity v of the fluorescent pulse was not constant, as in Luther's formula, but is rather expected to follow a diffusive scaling $v \sim 1/\sqrt{t}$. We thus anticipate that developing strategies to transfer DNA-rich information across membrane droplets will be an important question in the near future.

1.4. Steady-state spatial patterns

In the above we have discussed RD computations which output is time-dependent. However, in many instances a time-independent output is desirable. This is very challenging because diffusion will continuously dilute the output, so that reaction needs to balance diffusion to create a steady-state pattern. Steady-

state RD patterns are observed during early embryo development, where a robust output is needed. In addition, they can be useful to create synthetic morphogenetic materials with a chemically-defined final shape.

1.4.1. Colony formation

Inter-cellular communication is a critical parameter to precisely orchestrate tissue development and differentiation. In an attempt to emulate very primitively these communication channels between different objects, Gines et al. used DNA-programmed particles (cf. section 1.3.2.2) that exhibit synergism and cooperativity (Figure 1.8). The system uses two types of particles, P_{AB} and P_{BA}, that produce the output strand B from A, and conversely, using PEN reactions. The particules are dispersed in a solution containing the PEN exonuclease that degrades A and B, such that, when the particles are far from each other, homogeneous degradation is stronger than local particle production and no strand production is detected. However, when both particle types are present in close proximity, their cross-activation outcompetes degradation and both A and B are produced autocatalytically. The system evolves toward a steady-state where sharp concentration profiles are drawn around clusters of synergic particles, creating colony-like patterns in a large population of thousands of particles, which last for over dozens of hours. Interestingly, these colonies became more active as their density increased, suggesting long-distance interactions between the colonies that reinforce each other, in addition to the local synergic particle activation mechanism. Particle-based systems coupled to RD thus enable to easily control the topography of the reactions to start building large networks that display steady-state patterns. Although the par-

ticles used in this study were too big to remain suspended, Brownian particles would enable the exploration of 3D pattern formation.

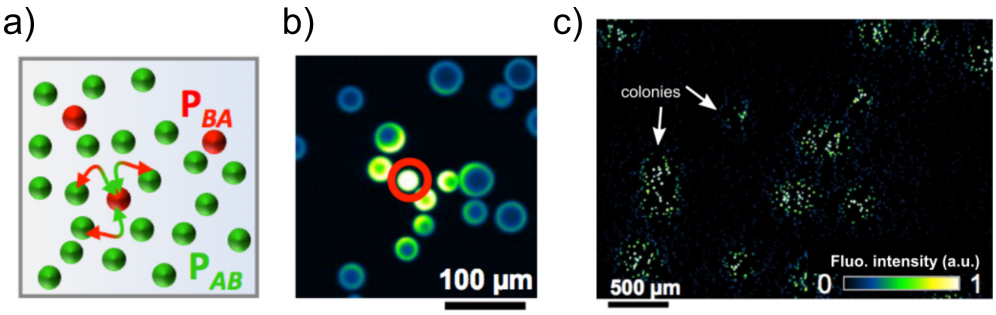

Figure 1.8: Steady-state 'colony' formation in a population of synergic particles functionalized with DNA templates. a) Red particles P_{BA} produce strand A in the presence of B and green particles P_{AB} produce B in the presence of A, through PEN reactions. b) When a red particle (circled in red) is present in close proximity to green particles, the emergent autocatalytic network outcompetes homogeneous degradation and forms a colony of high concentration of A and B (high fluorescence) at steady state. c) Large scale view of a small population of red particles dispersed among a large population of green particles. Colonies appear as clusters of green dots. Reprinted by permission from Springer Nature, Nature Nanotechnology, [20], Copyright 2017.

1.4.2. Patterns with positional information

The development of a living embryo is a fascinating process of spatial computation. Its early phase is called pattern formation and it is characterized by the generation of spatially-defined chemical concentration patterns. The principles underlying embryo pattern formation are still under debate[24], and they are largely dependent on the organism, the region and the developmental stage[69]. Nevertheless, two major conceptual frameworks have dominated our understanding of this process for the last 50 years[21]: Turing instability and positional information. The first one, developed by Turing in 1952[61, 60],

demonstrated that reaction-diffusion processes can form patterns. The second, introduced by Wolpert in 1969[70], proposed a simple way to explain how cells may compute their position within the embryo in the presence of a concentration gradient. The principal difference between the two is that the Turing instability is a symmetry-breaking mechanism that generates a heterogeneous concentration state from a homogeneous one, while positional information is a sharpening mechanism that amplifies a concentration heterogeneity from an initial state where the symmetry has already been broken. While patterns of positional information have recently been engineered with DNA networks[76, 80], DNA Turing patterns have yet to be demonstrated[79].

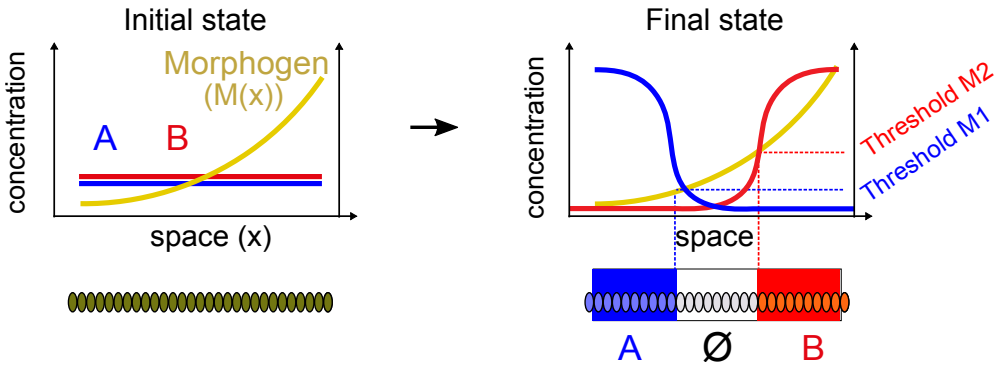

Figure 1.9: Illustration of Wolpert's concept of positional information as a solution of the 'French flag problem' in the presence of a shallow gradient of morphogen concentration in a 1-dimensional embryo.

The idea of positional information was introduced by Wolpert to explain how an embryo with a single break of symmetry could be further split into several distinct regions[70]. He coined the term 'French flag problem' to illustrate the challenge —fundamental because it is pervasive in the development of virtually all complex organisms— of creating three distinct regions of space with sharp borders from an amorphous mass and a shallow concentration gra-

dient. The idea of Wolpert is simple. Let's consider a model embryo formed by a 1-dimensional array of cells along the x axis submitted to an initial, monotonously decreasing, gradient of morphogen $M(x)$ (Figure 1.9). We suppose, for instance, that the cells on the left will become the head, those on the central part the thorax and those on the right the abdomen. In this situation, to know its position, each cell 'just' needs to read out the concentration of the morphogen along the gradient. Cells reading a concentration above a certain threshold $M(x) > M_1$ will express the blue protein, those below a second threshold $M(x) < M_2$ will express the red protein and those in between, the white protein (Figure 1.9). We say that the gradient provides *positional information* to the cells. Patterns generated by positional information were first observed in the *Drosophila* fly embryo [11, 10, 25]. They were engineered for the first time in vitro in a transcription-translation system by Isalan et al.[23]. In the following we will discuss recent DSD and PEN implementations of positional information patterns.

Zenk, Schulman and co-workers experimentally engineered static positional information patterns using DSD reactions[80]. In particular, they obtained linear and hill-shaped concentration patterns at steady state in an open gel reactor (Figure 1.10). To do so, a reaction network was designed to maintain the concentration of output strand O at steady state by a combination of rapid creation and slow degradation, as follows:

$$\mathrm{S} + \mathrm{I} \xrightarrow{k_1} \mathrm{O} + \mathrm{W}_1 \tag{1.7}$$

$$\mathrm{Rec} + \mathrm{O} \xrightarrow{k_2} \mathrm{W}_2 + \mathrm{W}_3 \tag{1.8}$$

where S and O are ssDNA and I and Rec are DSD gates with fast and slow

toeholds, respectively (i.e. $k_1 \gg k_2$). The reaction-diffusion pattern evolved in an open reactor composed of an agarose gel pad, about 1-cm long, connected on each side to a liquid reservoir in a linear geometry: reservoir/gel/reservoir. When the initial concentrations of both O and Rec where homogeneous in the three zones of the reactor but I and S were only present respectively in the left and right reservoirs, stable linear gradients of I and S appeared in the agarose pad, together with a stable hill-shaped profile of O. These patterns took about 30 h to form and lasted for about 70 h. Importantly, they could also be observed in 2D. Note that, due to the lack of a chemical sink, the liquid reservoirs needed to be replenished every 24 h to keep the system out of equilibrium. Finally, the authors demonstrated the programmability of their approach by engineering a second network, orthogonal with the initial one, that generated a second hill-shaped pattern. A related strategy was recently demonstrated by Chen and Seelig, obtaining more complex band patterns[7]. However, in this last case the patterns were generated in a closed reactor and thus they were not static.

A complementary approach to engineer static positional information patterns was demonstrated by Zadorin et al. using PEN reactions[76]. In particular, they obtained immobile RD fronts that could be assembled into a French flag pattern that produced three bands with distinct compositions. Their implementation is based on spatial bistability[46]: a bistable reaction network in the presence of a gradient of a species acting as a bifurcation parameter generates an immobile RD front.

PEN reactions may be assembled in a bistable network either by using two autocatalysts that cross-inhibit each other[40] (see Figures 1.3a and 1.5e) or one autocatalyst that is repressed by a saturable pathway[38]. In the last case the

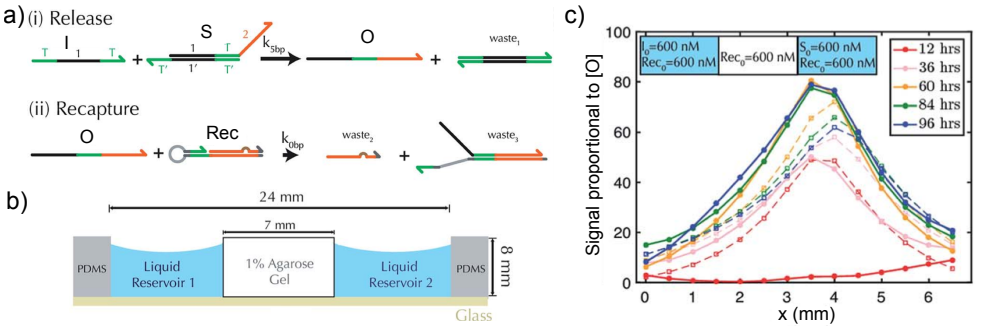

Figure 1.10: Static pattern of positional information engineered with DNA strand displacement circuits. a) Reaction mechanism of the DSD network used to maintain a steady-state concentration of strand O. b) Open gel reactor with liquid reservoirs on each side. The pattern is observed inside the gel pad. c) Dynamics of the hill-shaped pattern of species O obtained inside the gel reactor when the left reservoir contained species I, the right reservoir contained species S and Rec was distributed homogeneously. Adapted with permission from ref. 80. Published by The Royal Society of Chemistry.

network is composed of the autocatalytic production of A by its template T_{AA} (as in Fig. 1.5a), the degradation of A by the exonuclease and its repression by R_A that converts it into waste (see Figures 1.3a and 1.11a). This system is bistable because at low A, autocatalysis is slower than repression but at high A (typically $A > R_A$), the repression reaction saturates and shuts off. As a result the concentration of R_A acts as a bifurcation parameter.

Because PEN networks can be kept out of equilibrium for tens of hours in a closed reactor, implementing positional information is relatively straightforward: one just needs to fill a channel with a bistable network and generate a gradient of R_A along the channel (Figure 1.11b). The authors used a 5 cm-long glass capillary where a gradient of morphogen R_A was generated using Taylor dispersion[58, 62]. This way, the gradient was set up within minutes but remained stable for tens of hours, because diffusion over centimeter scales is very slow. With such an experimental setting, several multistable PEN net-

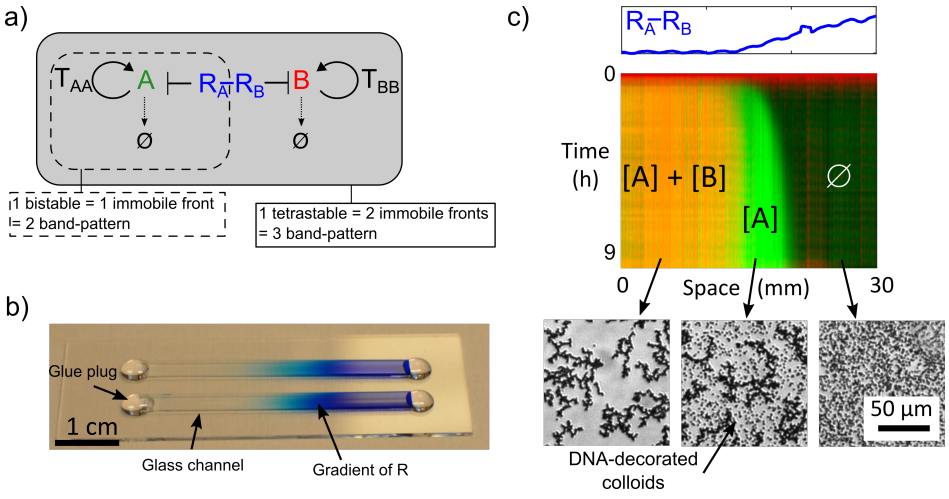

Figure 1.11: Static patterns of positional information can be engineered with PEN reactors and coupled to a simple material. a) Tetrastable network with autocatalytic nodes A, B and repressor R_A-R_B used to create a three band French flag pattern. Enclosed in dashed lines the bistable network that creates a two-band pattern. b) Photograph of the closed reactor where the patterns where obtained: a glass channel with a stable gradient of R_A-R_B (in blue). c) A tetrastable network in panel a forms a French flag pattern with three zones of different composition in the presence of a gradient of the corresponding repressor. The top image represents the stable underlying gradient concentration profile (in blue) and a kymograph of DNA fluorescence inside the channel. When the channel is initially filled with a homogeneous dispersion of DNA-decorated colloids, the reaction-network can be designed to specifically control the aggregation of the beads (bottom images). Reprinted by permission from Springer Nature, Nature Chemistry, [76], Copyright 2017.

works were tested with different repressor gradients, and a variety of steady-state band patterns were observed: an immobile front, two immobile fronts that repel each other and two immobile fronts that form a French flag pattern (Figure 1.11c). All the patterns self-organized in the same way: first a reaction-only phase generated a mobile front on the side of the channel where activation was stronger than repression, then the front(s) traveled through a reaction-diffusion mechanism towards the repression side, slowing down until a

RD steady-state was obtained. In addition, the borders of the bands were one order of magnitude sharper than the initial gradients (typically 1 mm compared with 1 cm). However, PEN autocatalytic parasites (see section 1.2.2.2) broke down the steady-state pattern after 10 h. This problem has recently been solved by constructing parasite-robust PEN networks[63] that are able to generate steady-state patterns that last for several days[62].

Pattern formation in the embryo is used for spatially-controlling subsequent developmental steps, such as cell differentiation. If we consider the embryo as a complex material and development as a self-fabrication process, the pattern would be the self-fabricated blueprint. Zadorin et al. emulated this idea in a very simple artificial system by coupling their PEN French flag pattern with the conditional aggregation of DNA-decorated colloids[76]. As a result, the DNA reaction-diffusion patterns just evoked differentiated an initially homogeneous material —a suspension of 1 μm colloids— into different zones with different microscopic structures (Figure 1.11c). Recently, Urtel et al. were able to maintain these band patterns at steady-state inside an autonomous hydrogel material[62], opening the way to building self-patterning autonomous materials.

1.5. Conclusion and perspectives

We have seen in this chapter that DNA circuits are well-suited to perform basic spatial computations. We have focused on computations that use reaction-diffusion primitives, which are the most natural operations that molecules perform in solution and, in particular, in illustrating their experimental implementations. The majority of DNA spatial computations involve analog circuits and

we have briefly discussed three of them: DNA strand displacement networks, genelets and PEN DNA reactions, all capable of generating oscillations in a closed reactor. DSD circuits have the advantage of being fully programmable because there are tools to predict the thermodynamics and kinetics of DNA hybridization reactions[85, 74, 34]. However, engineering 'chemical supplies' that maintain DSD networks out of equilibrium in a closed reactor is difficult. In this regard, DNA/enzyme networks, such as genelets and PEN reactions, are complementary to DSD: one needs to integrate the non-programmability of enzymes in the design process but, in exchange, maintaining the system out of equilibrium in a closed reactor is greatly facilitated. Although both DSD and DNA/enzyme approaches are both expected to be biocompatible (they run in aqueous buffer at pH 7 and 37 °C), the absence of enzymes in DSD networks may make them more widely compatible with biological systems containing biomolecules or living cells.

Autocatalytic nodes are a basic element of RD pattern formation because the exponential growth from autocatalysis balances the dilution arising from diffusion, creating traveling patterns. Autocatalysis can be easily implemented in PEN circuits and this has been used to demonstrate a series of non-trivial traveling patterns that are constructed around the principle of a traveling front[41, 75, 78, 76, 62]. Autocatalysis has been demonstrated in DSD circuits, but not for generating patterns, probably due to undesired leak reactions. However, recent strategies have succeeded in dramatically reducing leak in DSD reactions[55, 66], and thus autocatalytic DSD patterns may soon be observed. Instead, DSD patterns have explored other important network elements, such as incoherent feed forward loops[8] and steady-state generators[80]. In addition, the design of more complex DSD patterns[49] and of RD cellular

automata[48] has been illustrated through simulations, and we may soon see these realizations in experiments.

Now that the engineering of RD patterns with DNA programs has been thoroughly demonstrated, we see three interesting directions for future work. Firstly, to push forward the complexity of the engineered patterns. In this regard, an important objective is the engineering of Turing patterns, for which diffusion-control strategies[75, 43] evoked above are essential, and multi-phasic approaches[12] may also be advantageous. Secondly, the investigation of the fundamental mechanisms of molecular self-organization with DNA patterning systems. In particular, engineered patterns of positional information could help to ask questions about how developing embryos form patterns[21]. To succeed, this challenging approach will need a strong collaboration between DNA molecular programmers and developmental biologists. Finally, coupled to responsive DNA-materials[45, 16, 26, 5], DNA patterning systems could create a new generation of life-like materials capable of self-construction, communication and healing.

1.6. Acknowledgment

We thank Yannick Rondelez, Anton Zadorin, Adrian Zambrano, Georg Urtel, Anthony Genot and Nathanael Aubert for valuable discussions. This research has been supported by CNRS (J.C. G. and A.E.-T.), by the European Research Council (ERC) under the European's Union Horizon 2020 programme (grant No 770940, A.E.-T.), by the Ville de Paris Emergences programme (Morphoart, A.E.-T.), by a Marie Sklodowska-Curie fellowship (grant No 795580, M.V.D.H.) from the European Union's Horizon 2020 programme, by a PRES-

TIGE grant (grant No 609102, M.V.D.H.) from the European Union's Seventh Framework Programme, and by a PSL Research University fellowship (G.G).

Bibliography

[1] Keita Abe, Ibuki Kawamata, Shin-ichiro M. Nomura, and Satoshi Murata. Programmable reactions and diffusion using dna for pattern formation in hydrogel medium. *Molecular Systems Design & Engineering*, 4(3):639–643, 2019.

[2] Peter Allen, Xi Chen, and Andrew Ellington. Spatial control of dna reaction networks by dna sequence. *Molecules*, 17(11):13390–13402, 2012.

[3] Peter B. Allen, Xi Chen, Zack B. Simpson, and Andrew D. Ellington. Modeling scalable pattern generation in dna reaction networks. *Natural Computing*, 13(4):583–595, 2014.

[4] D. Bartolo, G. Degré, P. Nghe, and V. Studer. Microfluidic stickers. *Lab. Chip*, 8:274–279, 2008.

[5] Angelo Cangialosi, ChangKyu Yoon, Jiayu Liu, Qi Huang, Jingkai Guo, Thao D. Nguyen, David H. Gracias, and Rebecca Schulman. Dna sequence–directed shape change of photopatterned hydrogels via high-degree swelling. *Science*, 357(6356):1126–1130, 2017.

[6] Andrea Cavagna, Alessio Cimarelli, Irene Giardina, Giorgio Parisi, Raffaele Santagati, Fabio Stefanini, and Massimiliano Viale. Scale-free correlations in starling flocks. *Proceedings of the National Academy of Sciences*, 107(26):11865–11870, 2010.

[7] Sifang Chen and Georg Seelig. Programmable patterns in a dna-based reaction-diffusion system. *bioRxiv*, 2019.

[8] Steven M. Chirieleison, Peter B. Allen, Zack B. Simpson, Andrew D. Ellington, and Xi Chen. Pattern transformation with dna circuits. *Nat Chem*, 5(12):1000–1005, 2013.

[9] André DeHon, Jean-Louis Giavitto, and Fréderic Gruau. 06361 executive report – computing media languages for space-oriented computation. In André DeHon, Jean-Louis Giavitto, and Frédric Gruau, editors, *Computing Media and Languages for Space-Oriented Computation*, number 06361 in Dagstuhl Seminar Proceedings, Dagstuhl, Germany, 2007. Internationales Begegnungs- und Forschungszentrum für Informatik (IBFI), Schloss Dagstuhl, Germany.

[10] W Driever and C Nüsslein-Volhard. The bicoid protein determines position in the drosophila embryo in a concentration-dependent manner. *Cell*, 54:95–104, 1988.

[11] Wolfgang Driever and Christiane Nüsslein-Volhard. A gradient of bicoid protein in drosophila embryos. *Cell*, 54(1):83–93, 1988.

[12] Aurore Dupin and Friedrich C. Simmel. Signalling and differentiation in emulsion-based multi-compartmentalized in vitro gene circuits. *Nature Chemistry*, 11(1):32–39, 2019.

[13] I. Epstein and J. A. Pojman. *An introduction to nonlinear chemical reactions*. Oxford University Press, New York, 1998.

[14] I. R. Epstein and K. Showalter. Nonlinear chemical dynamics: Oscillations, patterns, and chaos. *J. Phys. Chem.*, 100(31):13132–13147, 1996.

[15] R. A. Fisher. The wave of advance of advantageous genes. *Ann. of Eugenics*, 7:355–369, 1937.

[16] Elisa Franco, Eike Friedrichs, Jongmin Kim, Ralf Jungmann, Richard Murray, Erik Winfree, and Friedrich C. Simmel. Timing molecular motion and production with a synthetic transcriptional clock. *Proc. Natl. Acad. Sci. U.S.A.*, 2011.

[17] Teruo Fujii and Yannick Rondelez. Predator-prey molecular ecosystems. *ACS Nano*, 7(1):27–34, 2013.

[18] A.J Genot., A. Baccouche, R. Sieskind, N. Aubert-Kato, N. Bredeche, J.F. Bartolo, V. Taly, T. Fujii, and Y. Rondelez. High-resolution mapping of bifurcations in nonlinear biochemical circuits. *Nat. Chem.*, 8:760–767, 2016.

[19] Anthony J. Genot, David Yu Zhang, Jonathan Bath, and Andrew J. Turberfield. Remote toehold: A mechanism for flexible control of dna hybridization kinetics. *J. Am. Chem. Soc.*, 133(7):2177–2182, 2011.

[20] G. Gines, A.S. Zadorin, J.-C. Galas, T. Fujii, A. Estevez-Torres, and Y. Rondelez. Microscopic agents programmed by dna circuits. *Nat Nano*, advance online publication:–, January 2017.

[21] J. B. Green and J. Sharpe. Positional information and reaction-diffusion: two big ideas in developmental biology combine. *Development*, 142(7): 1203–11, 2015.

[22] Fan Hong, Fei Zhang, Yan Liu, and Hao Yan. Dna origami: Scaffolds for creating higher order structures. *Chemical Reviews*, 117(20):12584–12640, 2017.

[23] M. Isalan, C. Lemerle, and L. Serrano. Engineering gene networks to emulate drosophila embryonic pattern formation. *PLoS Biol.*, 3(3):488–496, 2005.

[24] J. Jaeger, D. Irons, and N. Monk. Regulative feedback in pattern formation: towards a general relativistic theory of positional information. *Development*, 135(19):3175–83, 2008.

[25] Daniel St Johnston and Christiane Nüsslein-Volhard. The origin of pattern and polarity in the drosophila embryo. *Cell*, 68(2):201–219, 1992.

[26] Matthew R. Jones, Nadrian C. Seeman, and Chad A. Mirkin. Programmable materials and the nature of the dna bond. *Science*, 347(6224), 2015.

[27] J. Kim, K. S. White, and E. Winfree. Construction of an in vitro bistable circuit from synthetic transcriptional switches. *Mol. Syst. Biol.*, 2:68, 2006.

[28] Jongmin Kim and Erik Winfree. Synthetic in vitro transcriptional oscillators. *Mol. Syst. Biol.*, 7:465, 2011.

[29] A. Kolmogoroff, I. Petrovsky, and N. Piscounoff. Etude de l'equation de la diffusion avec croissance de la quantité de matiére et son application à un probleme biologique. *Bull. Univ. Moskou, Ser. Internat., Sec. A*, 6: 1–25, 1937.

[30] Shigeru Kondo and Takashi Miura. Reaction-diffusion model as a framework for understanding biological pattern formation. *Science*, 329(5999): 1616–1620, 2010.

[31] L. Kuhnert, K. I. Agladze, and V. I. Krinsky. Image-processing using light-sensitive chemical waves. *Nature*, 337(6204):244–247, 1989.

[32] Ievgen Kurylo, Guillaume Gines, Yannick Rondelez, Yannick Coffinier, and Alexis Vlandas. Spatiotemporal control of dna-based chemical reaction network via electrochemical activation in microfluidics. *Scientific Reports*, 8(1):6396, 2018.

[33] Martin Loose, Elisabeth Fischer-Friedrich, Jonas Ries, Karsten Kruse, and Petra Schwille. Spatial regulators for bacterial cell division self-organize into surface waves in vitro. *Science*, 320(5877):789–792, 2008.

[34] Ronny Lorenz, Stephan H. Bernhart, Christian Hner zu Siederdissen, Hakim Tafer, Christoph Flamm, Peter F. Stadler, and Ivo L. Hofacker. Viennarna package 2.0. *Algorithms for Molecular Biology*, 6(1):1–14, 2011.

[35] R. Luther. Space propagation of chemical reactions. *Zeitschrift Fur Elektrochemie Und Angewandte Physikalische Chemie*, 12:596–600, 1906.

[36] Robert Luther. Propagation of chemical reactions in space. *J. Chem. Educ.*, 64(9):740, 1987.

[37] Kevin Montagne, Raphael Plasson, Yasuyuki Sakai, Teruo Fujii, and Yannick Rondelez. Programming an in vitro dna oscillator using a molecular networking strategy. *Mol. Syst. Biol.*, 7:466, 2011.

[38] Kevin Montagne, Guillaume Gines, Teruo Fujii, and Yannick Rondelez. Boosting functionality of synthetic dna circuits with tailored deactivation. *Nat. Comm.*, 7:13474, 2016.

[39] J.D. Murray. *Mathematical Biology II :Spatial Models and Biomedical Applications*. Springer, New York, 2003.

[40] Adrien Padirac, Teruo Fujii, and Yannick Rondelez. Bottom-up construction of in vitro switchable memories. *Proc. Natl. Acad. Sci. U.S.A.*, 10.1073/pnas.1212069109, 2012.

[41] Adrien Padirac, Teruo Fujii, André Estévez-Torres, and Yannick Rondelez. Spatial waves in synthetic biochemical networks. *J. Am. Chem. Soc.*, 135 (39):14586–14592, 2013.

[42] Lulu Qian and Erik Winfree. Scaling up digital circuit computation with dna strand displacement cascades. *Science*, 332(6034):1196–1201, 2011.

[43] Thanapop Rodjanapanyakul, Fumi Takabatake, Keita Abe, Ibuki Kawamata, Shinichiro M. Nomura, and Satoshi Murata. Diffusion modulation of dna by toehold exchange. *Physical Review E*, 97(5):052617, 2018.

[44] Lionel Roques. *Modèles de réaction-diffusion pour l'écologie spatiale*. Editions Quae., Versailles, 2013.

[45] P. W. K. Rothemund. Folding dna to create nanoscale shapes and patterns. *Nature*, 440(7082):297–302, 2006.

[46] Steffen Rulands, Ben Klünder, and Erwin Frey. Stability of localized wave fronts in bistable systems. *Phys. Rev. Lett.*, 110(3):038102, 2013.

[47] Rahul Sarpeshkar. Analog versus digital: Extrapolating from electronics to neurobiology. *Neural Comput.*, 10(7):1601–1638, 1998.

[48] Dominic Scalise and Rebecca Schulman. Designing modular reaction-diffusion programs for complex pattern formation. *Technology*, 02(01): 55–66, 2014.

[49] Dominic Scalise and Rebecca Schulman. Emulating cellular automata in chemical reaction-diffusion networks. In Satoshi Murata and Satoshi Kobayashi, editors, *DNA Computing and Molecular Programming*, pages 67–83, Cham, 2014. Springer International Publishing.

[50] Dominic Scalise and Rebecca Schulman. Controlling matter at the molecular scale with dna circuits. *Annual Review of Biomedical Engineering*, 21(1):469–493, 2019.

[51] Samuel W. Schaffter and Rebecca Schulman. Building in vitro transcriptional regulatory networks by successively integrating multiple functional circuit modules. *Nature Chemistry*, 11(9):829–838, 2019.

[52] Georg Seelig, David Soloveichik, David Yu Zhang, and Erik Winfree. Enzyme-free nucleic acid logic circuits. *Science*, 314(5805):1585–1588, 2006.

[53] Friedrich C. Simmel and Rebecca Schulman. Self-organizing materials built with dna. *MRS Bulletin*, 42(12):913919, 2017.

[54] D. Soloveichik, G. Seelig, and E. Winfree. Dna as a universal substrate for chemical kinetics. *Proc. Natl. Acad. Sci. U. S. A.*, 107(12):5393–5398, 2010.

[55] Niranjan Srinivas, James Parkin, Georg Seelig, Erik Winfree, and David Soloveichik. Enzyme-free nucleic acid dynamical systems. *Science*, 358, 2017.

[56] Niranjan Srinivas, James Parkin, Georg Seelig, Erik Winfree, and David Soloveichik. Enzyme-free nucleic acid dynamical systems. *bioRxiv*, 2017. doi: 10.1101/138420.

[57] Alexandra M. Tayar, Eyal Karzbrun, Vincent Noireaux, and Roy H. Bar-Ziv. Propagating gene expression fronts in a one-dimensional coupled system of artificial cells. *Nat. Phys.*, advance online publication, 2015.

[58] G. I. Taylor. Dispersion of soluble matter in solvent flowing slowly through a tube. *Proc. R. Soc. A*, 219, 1953.

[59] A. J. Turberfield, J. C. Mitchell, B. Yurke, Jr. Mills, A. P., M. I. Blakey, and F. C. Simmel. DNA fuel for free-running nanomachines. *Phys. Rev. Lett.*, 90(11):118102, 2003.

[60] A. Turing. The chemical basis of morphogenesis. *Bull. Math. Biol.*, 52(1): 153–197, 1990.

[61] A. M. Turing. The chemical basis of morphogenesis. *Philos. Trans. R. Soc. Lond. B. Biol. Sci.*, 237(641):37–72, 1952.

[62] Georg Urtel, Andr Estevez-Torres, and Jean-Christophe Galas. Dna-based long-lived reaction-diffusion patterning in a host hydrogel. *Soft Matter*, in press, 2019.

[63] Georg Urtel, Marc Van Der Hofstadt, Jean-Christophe Galas, and Andr Estevez-Torres. rexpar: An isothermal amplification scheme that is robust to autocatalytic parasites. *Biochemistry*, 58(23):2675–2681, 2019.

[64] Wim van Saarloos. Front propagation into unstable states. *Phys. Rep.*, 386:29–222, 2003.

[65] V. Volpert and S. Petrovskii. Reaction–diffusion waves in biology. *Physics of Life Reviews*, 6(4):267–310, 2009.

[66] Boya Wang, Chris Thachuk, Andrew D. Ellington, Erik Winfree, and David Soloveichik. Effective design principles for leakless strand displacement systems. *Proceedings of the National Academy of Sciences*, 115(52): E12182–E12191, 2018.

[67] Siyuan S. Wang and Andrew D. Ellington. Pattern generation with nucleic acid chemical reaction networks. *Chemical Reviews*, 119(10):6370–6383, 2019.

[68] A. T. Winfree. Spiral waves of chemical activity. *Science*, 175(4022): 634–636, 1972.

[69] C. Wolpert, L.; Tickle. *Principles of development.* Oxford University Press, Oxford, 2011.

[70] L. Wolpert. Positional information and the spatial pattern of cellular differentiation. *J. Theor. Biol.*, 25(1):1–47, 1969.

[71] Yikang Xing, Bing Liu, Jie Chao, and Lianhui Wang. Dna-based nanoscale walking devices and their applications. *RSC Advances*, 7(75):47425–47434, 2017.

[72] Peng Yin, Harry M. T. Choi, Colby R. Calvert, and Niles A. Pierce. Programming biomolecular self-assembly pathways. *Nature*, 451(7176): 318–322, 2008.

[73] Bernard Yurke, Andrew J. Turberfield, Allen P. Mills, Friedrich C. Simmel, and Jennifer L. Neumann. A dna-fuelled molecular machine made of dna. *Nature*, 406(6796):605–608, 2000.

[74] Joseph N. Zadeh, Conrad D. Steenberg, Justin S. Bois, Brian R. Wolfe, Marshall B. Pierce, Asif R. Khan, Robert M. Dirks, and Niles A. Pierce.

Nupack: Analysis and design of nucleic acid systems. *J. Comput. Chem.*, 32(1):170–173, 2011.

[75] Anton S. Zadorin, Yannick Rondelez, Jean-Christophe Galas, and Andre Estevez-Torres. Synthesis of programmable reaction-diffusion fronts using dna catalyzers. *Phys. Rev. Lett.*, 114(6):068301, 2015.

[76] Anton S. Zadorin, Yannick Rondelez, Guillaume Gines, Vadim Dilhas, Georg Urtel, Adrian Zambrano, Jean-Christophe Galas, and André Estevez-Torres. Synthesis and materialization of a reaction-diffusion french flag pattern. *Nature Chemistry*, 9:990, 2017.

[77] A. N. Zaikin and A. M. Zhabotinsky. Concentration wave propagation in two-dimensional liquid-phase self-oscillating system. *Nature*, 225(5232): 535–537, 1970.

[78] A. Zambrano, A. S. Zadorin, Y. Rondelez, A. Estévez-Torres, and J. C. Galas. Pursuit-and-evasion reaction-diffusion waves in microreactors with tailored geometry. *The Journal of Physical Chemistry B*, 119(17):5349–5355, 2015.

[79] Adrian Zambrano. *Synthesis of reaction-diffusion patterns with DNA: towards Turing patterns.* Phd thesis, Université Paris-Saclay, 2016.

[80] John Zenk, Dominic Scalise, Kaiyuan Wang, Phillip Dorsey, Joshua Fern, Ariana Cruz, and Rebecca Schulman. Stable dna-based reaction-diffusion patterns. *RSC Adv.*, 7:18032–18040, 2017.

[81] D. Y. Zhang and E. Winfree. Control of dna strand displacement kinetics using toehold exchange. *J. Am. Chem. Soc.*, 131(47):17303–14, 2009.

[82] David Yu Zhang and Georg Seelig. Dynamic dna nanotechnology using strand-displacement reactions. *Nat Chem*, 3(2):103–113, 2011.

[83] David Yu Zhang, Andrew J. Turberfield, Bernard Yurke, and Erik Winfree. Engineering entropy-driven reactions and networks catalyzed by dna. *Science*, 318(5853):1121–1125, 2007.

[84] Katja Zieske, Petra Schwille, and Mohan Balasubramanian. Reconstitution of self-organizing protein gradients as spatial cues in cell-free systems. *eLife*, 3:e03949, 2014.

[85] Michael Zuker. Mfold web server for nucleic acid folding and hybridization prediction. *Nucleic Acids Res.*, 31(13):3406–3415, 2003.

[86] Nadezhda V. Zyrina, Valeriya N. Antipova, and Lyudmila A. Zheleznaya. Ab initio synthesis by dna polymerases. *FEMS Microbiology Letters*, 351 (1):1, 2014.